DevoWorm: data-theoretical synthesis of *C. elegans* development

Bradly Alicea[1,2], Richard Gordon[3,4], Thomas E. Portegys[1,5]

[1]OpenWorm Foundation, Boston MA; [2]Orthogonal Research Lab, Champaign, IL; [3]Gulf Marine Specimen Laboratory, Panacea, FL; [4]C.S. Mott Center for Human Growth and Development, Department of Obstetrics and Gynecology, Wayne State University, Detroit MI; [5]EY Consulting, Seattle, WA

Keywords: Developmental Biology, Computational Biology, Artificial Life, *Caenorhabditis elegans*

ABSTRACT

The DevoWorm group adds an important dimension to the OpenWorm Foundation's goal of creating a digital nematode. Compared with the great diversity and plasticity found across the tree of life, *Caenorhabditis elegans* development is a rather unique model system. *C. elegans* biology provides us with a highly-deterministic developmental cell lineage, and a clear linkage from zygote to cells of the adult phenotype. This paper provides an example of the DevoWorm approach, merging computational modeling and insights from data science. The first part introduces alternative ways of understanding the embryo, including the role of hierarchical differentiation and whole-embryo pattern generation. We suggest that systematic decomposition of embryo feature space is just as important to understanding the embryo as single-gene and molecular studies.

The second half of this paper focuses on the process of developmental cell terminal differentiation, and how terminally-differentiated cells contribute to structure and function of the adult phenotype. An analysis is conducted for cells that were present during discrete time intervals covering 200 to 400 minutes of embryogenesis, providing us with basic statistics on the tempo of the embryogenetic process in addition to the appearance of specific cell types and their order relative to embryogenetic time. As with ideas presented in the first section, these data may also provide clues as to the timing for the initial onset of stereotyped and autonomic behaviors of the developing animal. Taken together, these overlapping approaches can provide critical links across life-history, anatomy and function to reveal the essential components needed to create a complex digital organism, where artificial life imitates real life.

Introduction

The DevoWorm group [1] was founded in early 2014, initially focused on acquiring secondary data to produce data structures and tree structures to describe the process of differentiation in the *Caenorhabditis elegans* embryo [2]. As our access to more and various

types of data expanded, we added a more diverse set of methods including cellular automata, experimental evolution, and comparative embryogenesis. DevoWorm is nominally divided into three interest areas: a) developmental dynamics, b) cybernetics and digital morphogenesis, and c) reproduction and developmental plasticity. This provides significant linkage to OpenWorm's other projects which focus on the adult worm.

A meta-interest of the DevoWorm group is understanding the role of biological complexity in *C. elegans* development and consequences for building a digital worm. Whether the relatively simple development of the nematode phenotype or that of vertebrates is being considered, it is difficult to link the embryogenetic process to the adult phenotype. To overcome this limitation of more traditional developmental research, we have engaged in work that advances the concept of a differentiation tree [3, 4]. In nematodes differentiation trees are a means to relate the binary, mostly asymmetric cell divisions to the broader context of embryonic tissue differentiation. This provides us with a means by which to explore comparisons between developmental cell lineages that define specific genotypes, as well as changes that define the evolution of development (see Figure 1). Specifically, the *information isometry* technique [4] allows us to determine whether a set of lineage changes is due to random chance or is a product of controlled asymmetries.

The rest of this section will focus on the role of analysing development and computation/development. This serves to lead into the second section, in which we synthesize data analysis and visualization. In this case, the analysis of development is revisited with a specific case study presented using secondary data.

Analysis of Development

In this section, we will discuss current initiatives and future directions in the analysis of development. This includes a discussion of developmental cell organization, and overview of developmental cell lineage and differentiation trees, segmentation/partitioning of imaging data, and the extraction of developmental dynamics.

Developmental Cell Organization

C. elegans has a specialized mode of development called *mosaic development*. While this is different from embryonic *regulative development* in amphibians and mammals, in which many cells appear to have equivalent roles [11], there are many other examples of *mosaic development* throughout the tree of life. Mosaic development is a process whereby most developmental cells are fate deterministic. After the initial cleavages in *C. elegans*, there are six founder cells (*AB*, *C*, *D*, *E*, *MS*, *P4*) which go on to produce specialized lineages of cells with no variation across individuals. Upon terminal differentiation, these sublineages contribute to various tissue and anatomical structures in

the adult worm. *C. elegans* is eutelic, which means that there is a fixed number of somatic cells in the adult.

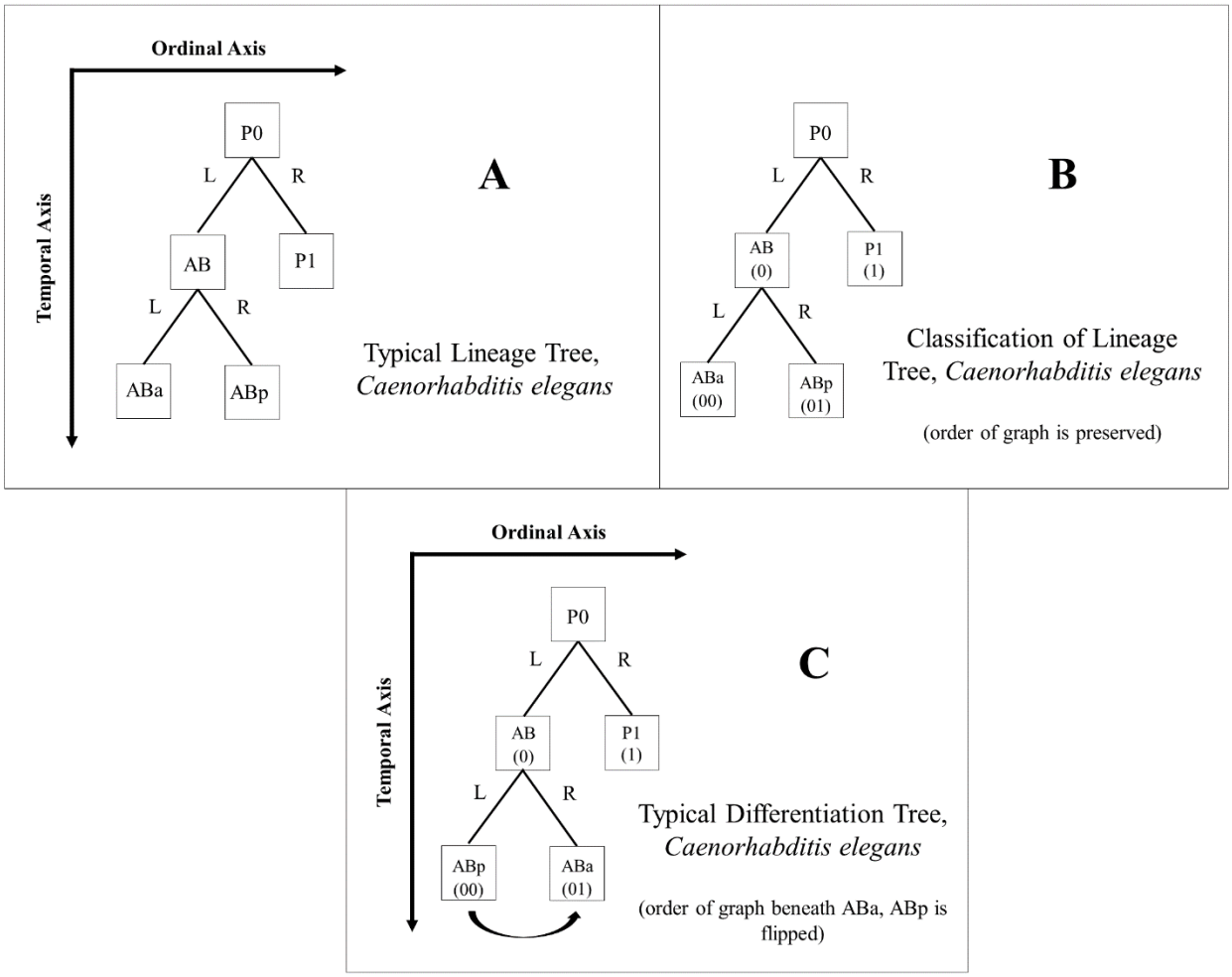

FIGURE 1. Diagram of the difference between a Lineage Tree and a Differentiation Tree (Adapted from [3] with permission under a Creative Commons Attribution (CC-BY) license). A) the ordinal and temporal organization of a typical lineage tree in *C. elegans*, B) classification of the lineage tree using the anterior-posterior order as the basis for a binary classification of nodes, C) the ordinal and temporal organization of a typical differentiation tree, reclassified as a series of contraction and expansion waves (based on daughter cell size, i.e., asymmetric cell division producing a smaller cell, placed to the left, and a larger cell, placed to the right). See [11] for the relationship between differentiation waves and asymmetric divisions.

Developmental Cell Lineage Tree

The *C. elegans* lineage tree [5] describes the lineal order of descent for all developmental cells from the one-cell stage to terminal differentation. The lineage tree is ordered along the Anterior-Posterior axis of the worm [6], and describes the lineage of descent for all cells in the adult worm. Sublineages (descendants of the founder cells) consist of multiple layers of cells, which diversify at fixed times before giving birth to

terminally differentiated cell types, also at fixed times. The timings of these division events are rather uniform across layers of the tree, although there are some notable exceptions.

Developmental Cell Differentiation Tree

Lineage trees have been proven to be adequate data structures for organizing information about developmental cell descent. However, other intriguing sets of relationships between developmental cells exist, and require different modes of data organization and analysis. Alternative methods include meta-Boolean models [7], complex networks [8], algorithmic complexity [9], and scale-invariant power laws [10]. One method that relies upon simply reorganizing the lineage tree by the occurrence of differentiation waves is called differentiation tree analysis [11]. We have visualized the process behind how a differentiation tree forms in the context of embryonic anatomy in Supplemental Figure 1. Differentiation waves involve propagation of either a contraction or expansion of the apical surfaces of cells in a given epithelial tissue. In the case of mosaic development (such as in the case of *C. elegans*), tissues are replaced with individual cells. In other words, an asymmetric cell division involves both a single-cell contraction wave, resulting in the smaller cell, accompanied by a single-cell expansion wave, resulting in the larger cell. An exception to this involves the small proportion of the cell divisions in *C. elegans* are symmetric, resulting in tissues containing two cells [11]. This set of rules allows us to bring regulative and mosaic development under one theory, the difference being that in regulative embryos tissues consist of many cell, whereas in mosaic embryos tissues consist of one cell.

Segmentation/Partitioning and Extraction of Developmental Dynamics

One way we collect data is to apply computer vision techniques to microscopy data. This can be done using various criteria ranging from thresholding and boundary discovery to more computationally extensive machine learning techniques. This allows us to evaluate the geometry of individual cells as well as their relationship to the geometry of the whole embryo.

Aside from alternative representations of the developmental process, the DevoWorm group is also interested in extracting developmental dynamics (time series) from secondary data sources. Specifically, we have established a dataset that links developmental cell lineages with terminally-differentiated cells annotated with their function and location in the adult phenotype.

Computation and Simulation

In this section, we will discuss approaches to the computational and representational modeling of development. The DevoWorm group has been engaged in two parallel approaches: digital morphogenesis, cellular-level models, both as alternatives to

reductionism. We will also highlight generative approaches to be developed as next steps in the project. These include visualization via the *k-D* embryo and a Voronoi treemap implementation of the developmental process.

Digital Morphogenesis

The DevoWorm group is also involved in modeling the self-organization of biological systems. Focusing on the cellular level, we have been able to approximate the shape and formation of complex multicellular structures. For example, we have introduced a hybrid cellular automata-neural network model called Morphozoic [12]. Morphozoic allows for nested two-dimensional neighborhoods (Moore neighborhoods nested inside of Metamorphs) to discover patterns in input data. The neural network component functions as an unsupervised classifier of the discovered patterns. Morphozoic has been trained on images of embryo data, and can form shapes on a grid that are similar to patterns observed in developmental, such as gastrulation. Further development of this technique is embodied in Morphognostic [13], a technique in which disembodied cognition is modeled as blocks of space-time. This cognitive engine can work to find patterns in a manner similar to Morphozoic.

We have also explored ways to use CompuCell3D [14, 15], a Cellular Potts model that provides a realistic view of dynamic embryo physics. This stands as a future direction for the project, in particular running realistic simulations of developmental processes in the embryo.

Cellular-level Alternatives to Reductionism

Through the use of cellular-level computational models, we can account for short-range interactions such as paracrine signaling and physical interactions. We can also combine the results from simulation and primary datasets into a model of selective interactions between cells and regions of the embryo. Our work on establishing an "interactome" for *C. elegans* embryos [8] is an example of the value of such local-to-global information. There is also value in establishing frameworks for multiple types of data, which might lead to inference or insight down the road. The existence of both molecular and cellular data at the single cell level in *C. elegans* provides a unique opportunity to ask questions such as how the physiology of embryogenesis unfolds in space.

Visualization via the *k-D* Embryo

Another way to segment the embryo is to decompose the lineage tree using computational techniques. As the lineage tree serves as a relatively compact computational representation of the embryo, any decomposition of this tree should serve to extract hidden structure in the embryogenetic process. We propose that a *k-D* tree decomposition can be used to discover structural features in tissue growth [16] along with

serving as a bridge to additional data visualization. This would provide us with a system of addressable data corresponding to specific cells and cell linages.

Voronoi Treemaps

As the *k-D* embryo is addressable, it provides us with a means to create novel visualizations of the data. One such means is a version of *k-D* partitioning called a Voronoi treemap [17-21]. First introduced in 2005 [17], a Voronoi treemap partitions the data recursively to find the optimal set of partitions in a spherical space. Voronoi treemaps and Voronoi diagrams more generally have been applied to the study of embryogenesis [18] and biodiversity [19]. This provides an opportunity to merge the developmental biology of a model organism with an emerging computational technique [20, 21].

Synthesis of Data and Visualization

Patterns of differentiation provide a means to determine the emergence of function in embryogenesis. In the model organism *C. elegans*, a deterministic developmental trajectory [22, 23] combined with available secondary data can be used to determine when terminally-differentiated cells appear and their relationship to both cell lineages and the adult phenotype. In this paper, we will ask the following question: in what order do distinct cells emerge within and between tissue types at multiple time points in pre-hatch morphogenesis? These data can provide insights into how movement and other behaviors first turn on, such as in cases where a specific cell is required for a generalized behavior or response [24]. In general, there is a great deal known about why the temporal emergence of *C. elegans* tissues and organs from terminally-differentiated cells is tightly regulated. However, a systems-level analysis and visualization of these cells could allow us understand which cell types and anatomical features are necessary and/or sufficient for the emergence of autonomic behaviors and functional phenotypes.

In *C. elegans*, cell division patterns directly correspond to cell fate [25]. Furthermore, the timing and ordered emergence of cells making up a specific tissue or organ is highly regulated at the molecular level. Heterochronic timing and associated heterochronic genes are major drivers of *C. elegans* embryogenesis, particularly since the developmental process is more discrete than in vertebrates [26]. Cellular behaviors such as reorientation and contraction accompany the multi-step morphogenesis of anatomical structures such as the pharynx [27]. The coordination of cell division timing is a complex relationship related to developmental timing, and leads to asynchrony of divisions between sister cells [28]. The pace of cell division itself is an important regulator critical for the normal formation of tissues and organs [29]. The failure of normal development outside a specific temperature range, such as has been observed in amphibians [30], could be investigated in *C. elegans* at the single cell level.

This time-dependent type of single-cell developmental regulation has consequences for differentiated cells that comprise specific tissues and organs. For example, every cell has a unique pattern of transcriptional regulation in embryonic development [31]. The dynamic regulation of each developmental cell [32] leads to differentiated cells with diverse functions [33]. A key to better understanding the coordination of cellular differentiation in development is to look at differential transcription within and between cells [34]. The timing of cell division and differentiation events appear to influence which parts of a tissue or organ form before others and ensure proper function [34]. There is also a functional role for certain types of cells, which thus must be present at a certain stage of embryogenesis for proper anatomical function and the onset of behaviors. For example, glial cells are all purpose cells that play a critical role in the onset of movement and autonomic behaviors [35]. The presence, and more importantly absence, of actin molecules in cells that make up certain anatomical structures can affect their formation and function [36].

Data and Visualization – Results

We conducted an analysis of publically available data demonstrating the unfolding of adult morphology during embryogenesis. The methods for this analysis and information about data availability are provided in Supplemental File 1. The first step in the analysis is to show the number of developmental and terminally-differentiated cells from 200-400 minutes. These data are available in tabular form for annotated nomenclature identities (Supplemental File 2) and for five distinct somatic cell types (Supplemental File 3). Supplemental Figure 2 demonstrates, not surprisingly, that the total number of cells in the embryo increases over time. Perhaps more surprisingly is that developmental cells are added along with an increasing number of terminal-differentiation cells until around 250 minutes of embryogenesis. At around the same time, there is an inflection point for developmental cell number and an increase in the number of terminally-differentiated cells in the embryo.

As a more finely sampled demographic representation of the 200-300 minute interval shown in Supplemental Figure 2, Figure 2A, shows that the number of cells increases 2.5-fold over that 100 minute interval. In general, Figure 2 also provides two critical pieces of information about developmental dynamics. The first of these suggests a periodicity in the rate of expansion in the number of cells of the embryo. In Figure 2A, it appears that there are periods of relative stasis and periods where the rate of division and differentiation increase. One of these apparent periods of stasis is from 235 to 270 minutes for terminally-differentiated cells, and 245 to 270 minutes for all cells. This includes both developmental and terminally-differentiated cells, so the difference in stasis time is likely due to changes in developmental cell number.

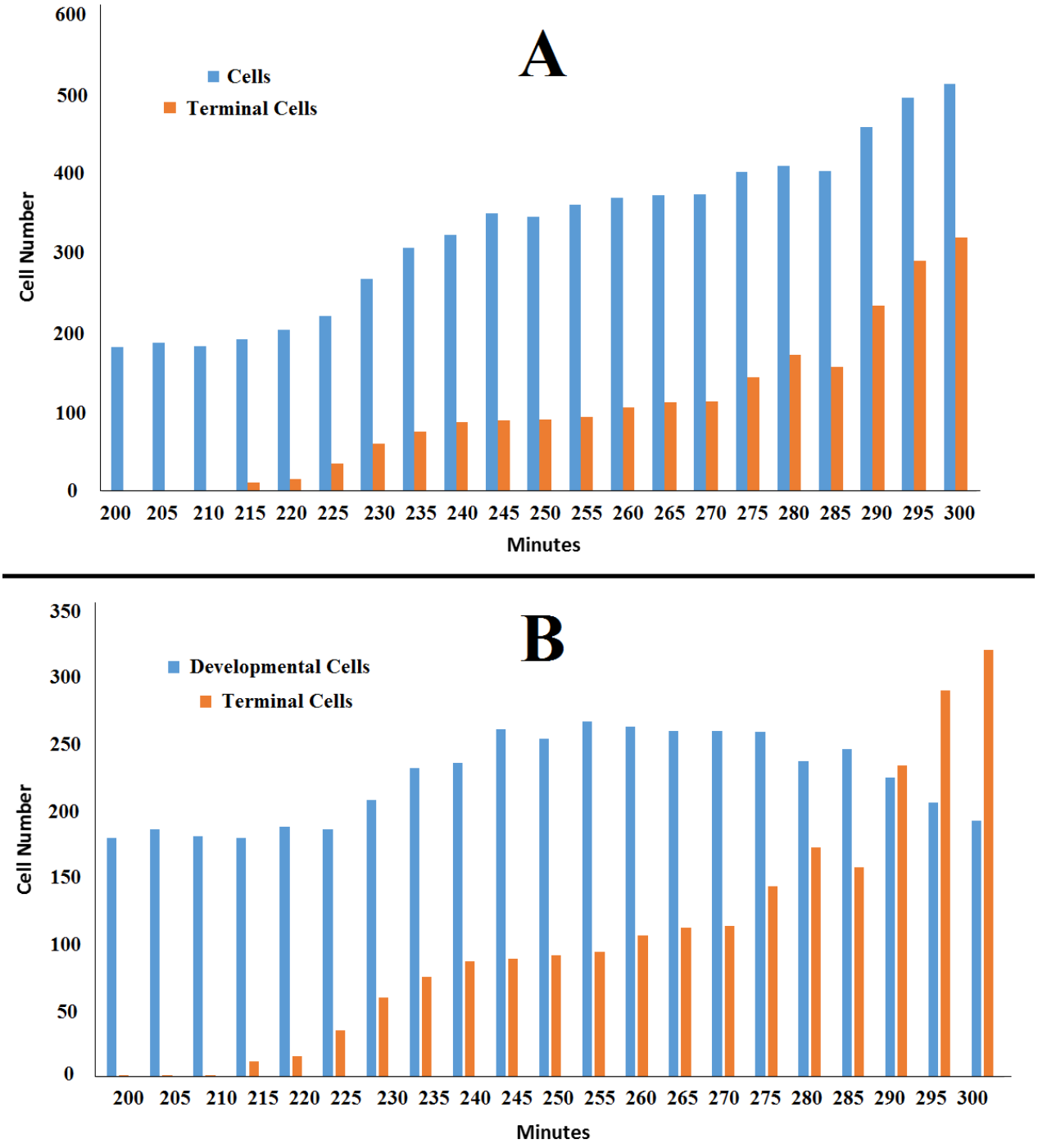

FIGURE 2. The ratio of all cells to terminally-differentiated cells (A, top) and developmental cells to terminally-differentiated cells (B, bottom) at 5 minute intervals from 200 to 300 minutes of embryogenesis.

The second piece of information in Figure 2 involves a demonstration of how the number of terminally-differentiated cells exceeds the number of developmental cells in the period from 285 to 290 minutes (Figure 2B). After 285 minutes, the *C. elegans* embryo is increasingly dominated by terminally-differentiated cells, as the number of developmental

cells decreases. There are roughly the same number of developmental cells at the beginning and end of this time interval. However, in the middle of this interval (from roughly 230 to 285 minutes), there is an increase in the number of developmental cells. This is probably to feed the large increase in terminally-differentiated cells in the subsequent time periods (from roughly 285 to 350 minutes).

Supplemental Figure 3 demonstrates these changes in the number of developmental cells, but is broken out by sublineage. In Figure 3A, we demonstrate both the number of cells in AB and MS, and the transient increase in developmental cells for sublineages AB and MS. Supplemental Figure 3B shows the number of cells in the C, D, and E sublineages. Interestingly, the fluctuation pattern demonstrated in Supplemental Figure 3A does not occur in sublineage C, and is hard to identify in sublineages D and E (Supplemental Figure 3B).

Next we turn to changes in the number of terminally-differentiated cells over time, particularly as broken down by specific cell families (e.g. nomenclature identities sharing the same prefix). In Figure 3, we can see that increases in the number of cells in each family differ in both rate of increase and time of origin. Hypodermal (*hyp*) cells begin to terminally-differentiate first, followed amphid (*AD*), inner labial (*IL*), and intestinal (*int*) cells. Up to 300 minutes, the majority of cells of the subsample in Figure 6 are hypodermal and intestinal cells. Using 200 minutes as a baseline for the earliest possible terminal differentiation, *hyp*, *AD*, *IL*, and *int* cells are what we consider to be early emerging cells.

While different terminally-differentiated cell families emerge at different times (Supplemental File 4), a more relevant question with respect to organ and tissue formation is how do different co-functional cell types compare in terms of their rate and time of differentiation. In Supplemental Figure 4, this question is answered for two separate comparisons of co-functional cell families using histograms. In Supplemental Figure 4A, we compare neurons and interneurons. Meanwhile, Supplemental Figure 4B compares interneurons and hypodermal cells. In the case of Supplemental Figure 4A, neurons merge in a bimodal fashion (with a majority of terminally-differentiated neurons being born from 290-400 minutes). By contrast, interneurons seem to almost always emerge after 280 minutes. Critically, there is an overlap in terms of terminal-differentiation between the two cell types. This may reveal an interdependency between the two cell types. By contrast, Supplemental Figure 4B shows a difference in mode between interneurons and hypodermal cells, with their frequency of emergence being almost inverse with respect to the 200 to 400 minute time interval.

These data can also be represented in the form of an annotated heat map (Supplemental Figure 5). The heat map in Supplemental Figure 5 contains all terminally-

differentiated cells present up to 400 minutes of embryogenesis. Each color represents a specific nomenclature identity which corresponds to the specific functional class (e.g. neuron, hypodermal, muscle) of an individual cell. Supplemental Figures 6 (Hypodermal and Interneuronal), 7 (Neuronal and Syncytium), and 8 (Muscle and Synticium) show subsets of the main heat map contiguously, which compares two classes of terminally-differentiated cell in a continuous fashion. It is of note that Supplemental Figure 6 is a more detailed representation of the comparison found in Supplemental Figure 3B.

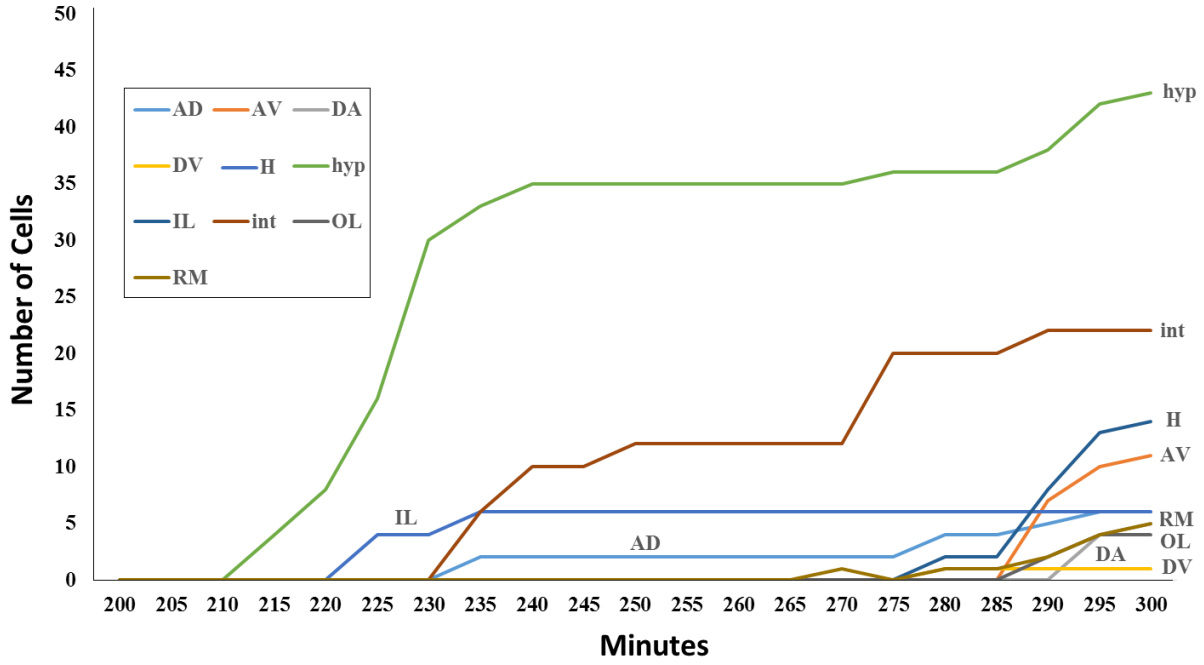

FIGURE 3. Number of cells for selected families of terminally-differentiated cells for 5-minute intervals over 200-300 minutes of embryogenesis. *AD* = Amphid cell, anterior deirid; *AV* = *Neurons*, interneurons; *DA* = Ventral motorneuron; *DV* = Ring interneurons; *H* = Seam hypodermal cell; *hyp* = Hypodermal cells; *IL* = Inner labial; *int* = Intestinal cell; *OL* = Outer labial; *RM* = Ring motorneuron/interneuron.

The heat map visualization gives us a rough guide to the amount of heterogeneity in each functional class with respect to time of birth. For some functional classes (nomenclature identity "*h*"), the birth of cells overwhelmingly occurs early in the 200 to 400 minute window of development. In other functional classes (nomenclature identity "*i*"), there is structured variation with respect to birth time. A third set of functional classes (nomenclature identities "*A*" and "*M*") also demonstrate variation in timing between cells. Table 1 shows the descriptive statistics for each family and functional class of cell present in the embryo up to 400 minutes of embryogenesis.

The "Interneuron" functional class in Supplemental Figure 6 shows the phenomenon of structured variation in more detail. In the heat map, the emergence of

cells at different points in time look like jagged teeth across the cell identity (vertical) axis. This represents the birth of axial variants of the same cell type at slightly different points in time. Looking more closely at axial variants with the same identity, we can see that while some axial variants emerge at the same time (e.g. *AIAL* and *AIAR*, right/left homologues of amphid interneurons), others emerge 5-15 minutes apart. Examples of these include *SMBDL* and *SMBVL* (dorsal/ventral homologues of ring/ motor interneurons) and *RIPR* and RIPL (right/left homologues of ring/pharynx interneurons). Supplemental Figure 8 shows the relationship between syncytium and muscle cells. For the most part, syncytium emerges earlier in time than do muscle cells. However, there is a group of embryonic body wall (*mu bod*) cells born just after the first wave of syncytia. More closely resembling the timing of neuronal cells in Supplemental Figure 7, these syncytia differentiate much earlier than the other embryonic body wall cells in our dataset.

We can also look at the relationship between the time of birth and number of cells per functional class. To discover patterns in these data, we conducted a hierarchical cluster analysis on the birth times for each terminally-differentiated cell. Supplemental File 4 provides an overview of the relationship between cluster membership and nomenclature family. This provides us with a set of 17 distinct clusters which we can use to classify each cell. Supplemental File 5 shows a table with all functional classes of terminally-differentiated cells and their average time of birth up to 400 minutes of embryogenesis. We asked whether cells from the same nomenclature family belonged to the same cluster. Supplemental Figure 9 shows the variation in information content across nomenclature families. The closer the value is to 1.0, the greater the information (e.g. cells from a single family are represented in a greater number of clusters).

Supplemental Figure 9 demonstrates that there are four types of nomenclature families: 1) relatively high information content with few members, 2) relatively low information content with few members, 3) relatively high information content with many members, and 4) relatively low information content with many members. This can be determined quantitatively by classifying the families based on whether their information content and cell number is above or below the median value of each. Using this method, we can determine the number of families in each category and their exemplars. Exemplars of Type 1 (1 family out of 26) include family U. Exemplars of Type 2 (12 families out of 26) include families B, E, G, and rect. Exemplars of Type 3 (11 families out of 26) include families D, M, mu, and V. Exemplars of Type 4 (1 family out of 26) include family C.

Finally, we can examine the series of terminally-differentiated cells that emerge at different time points as a CAST alignment [15]. CAST alignments provide an assessment of gaps in series of functionally-related cells as well as potential periods of stasis in the differentiation process (Supplemental File 6). Supplemental Figure 10 shows us the pattern

for the 200 to 400 minutes of *C. elegans* embryogenesis time-series. In this time-series, we see a large fluctuation in the CAST coefficient between the 205-210 minute interval and the 240-245 minute interval. There are subsequent fluctuations in the CAST coefficient that become increasing sharp after the 240-245 minute interval. This may be due to a transient period of stasis in differentiation shown in Figure 2.

Data and Visualization – Discussion

We have presented an analysis and visualization of cellular differentiation at a critical time period in *C. elegans* embryogenesis. The 200 to 400 minute interval is the time between the first appearance of non-germline terminally-differentiated cells and the comma stage of development [37]. It is during the first part of this time period that the major differentiated cell categories are established. This has been done by looking at the ratio of developmental cells to terminally-differentiated cells, looking at the different cell families and the relative timing of their differentiation, and variation in timing within and between functional classes.

Looking between functional classes also reveals information about how larger-scale structures are built (e.g. nervous system). For example, Supplemental Figure 4 shows the relationship between interneurons and neurons (A) and interneurons and hypodermal cells (B). In Supplemental Figure 4A, the appearance of neurons is multimodal with respect to time (one early group and a larger latter group). By contrast, almost all interneurons appear after 275 minutes. The timing of hypodermal cells is even more striking in comparison to interneurons as shown in Supplemental Figure 4B. In this case, a large group of hypodermal cells appear before the sampled interneurons, while a smaller group of hypodermal cells appear alongside the sampled interneurons. These types of comparisons can provide clues as to the emergence of organs as well as other functional networks of cells (connectome).

The first consideration for further study is the behavioral relevance of structured differentiation. As autonomic (e.g. pharyngeal pumping) and other basic behaviors emerge from the developing embryo [38], we can ask questions regarding the minimal set of cells required for initiation of a given behavior, the appearance of cells essential to turning on that behaviour, and whether or not behavioural emergence involves more than terminally differentiated cells.

The second consideration is how the process of development can be represented as a spatiotemporal process. While this is foremost a data visualization problem, it is also critical in showing how the adult phenotype is modular with respect to developmental time. In a number of cases, we can observe a multitude of its components terminally differentiated well before the initiation of function.

Summary

With over 50,000 articles listed in Web of Science on *C. elegans*, data mining and data analysis and visualization is a practical approach to understanding how this worm builds itself. Our concept of the differentiation tree as an alternative to the lineage tree provides a starting point. While we have not arrived at any grand conclusions, the analyses here provide some tantalizing hints that we, and hopefully others, will follow up on. In particular, we may now have the tools to start dissecting the development of behavior in this model organism.

Acknowledgments

We would like to acknowledge feedback from the OpenWorm and DevoWorm communities, particularly Drs. Stephen Larson, George Mikhailovsky, and senior contributors at the OpenWorm Foundation.

Authors' Contributions

Manuscript was written by B.A., and revised by R.G. and T.E.P. Figures and tables were created and assembled by B.A., with input from R.G. Analysis was conducted by B.A. Ideas and conception for manuscript were done by B.A., R.G., and T.E.P. Data archival was done by B.A.

Competing Interests

We have no competing interests.

Funding

No external funding sources were used to write this paper or conduct the studies herein.

REFERENCES

1. Website: http://devoworm.weebly.com.

2. Alicea, B., McGrew, S., Gordon, R., Larson, S., Warrington, T., and Watts, M. (2014). DevoWorm: differentiation waves and computation in *C. elegans* embryogenesis. bioRxiv, doi:10.1101/009993.

3. Alicea, B. and Gordon, R. (2016). Quantifying Mosaic Development: Towards an Evo-Devo Postmodern Synthesis of the Evolution of Development Via Differentiation Trees of Embryos. Biology (Basel), 5(3), 33.4.

4. Alicea, B., Portegys, T.E., and Gordon, R. (2016). Information Isometry Technique Reveals Organizational Features in Developmental Cell Lineages. bioRxiv, doi:10.1101/062539.

5. Sulston, J.E., Schierenberg, E., White, J.G., and Thomson, J.N. (1983). The embryonic cell lineage of the nematode *Caenorhabditis elegans*. Developmental Biology, 100(1), 64-119.

6. Bao, Z., Murray, J.I., Boyle, T., Ooi, S-L., Sandel, M.J., and Waterston, R.H. (2006). Automated cell lineage tracing in *Caenorhabditis elegans*. PNAS, 103(8), 2707–2712.

7. Pettersson, S., Forchheimer, R., and Larsson, J-A. (2013). Meta-Boolean models of asymmetric division patterns in the *C. elegans* intestinal lineage Implications for the posterior boundary of intestinal twist. Worm, 2(1), e23701.

8. Alicea, B. and Gordon, R. (2018). Cell Differentiation Processes as Spatial Networks: identifying four-dimensional structure in embryogenesis. PeerJ Preprints, 6, e26587.

9. Azevedo, R.B.R., Lohaus, R., Braun, V., Gumbel, M., Umamaheshwar, M., Agapow, P.M., Houthoofd, W., Platzer, U., Borgonie, G., Meinzer, H.P., and Leroi, A.M. (2005). The simplicity of metazoan cell lineages. Nature, 433, 152–156.

10. Tiraihi, A., Tiraihi, M., and Tiraihi, T. (2011). Self-organization of developing embryo using scale-invariant approach. Theoretical Biology and Medical Modeling, 8, 17.

11. Gordon, R. (1999). The Hierarchical Genome and Differentiation Waves: Novel Unification of Development, Genetics and Evolution. World Scientific, Singapore.

12. Portegys, T., Pascualy, G., Gordon, R., McGrew, S., and Alicea, B. (2016). Morphozoic: cellular automata with nested neighborhoods as a metamorphic representation of morphogenesis. In "Multi-Agent Based Simulations Applied to Biological and Environmental Systems", IGI Press, 44-80.

13. Portegys, T.E. (2017). Morphognosis: the shape of knowledge in space and time. arXiv, 1701.02272.

14. Nakamoto, A., Hester, S.D., Constantinou, S.J., Blaine, W.G., Tewksbury, A.B., Matei, M.T., Nagy, L.M., and Williams, T.A. (2015). Changing cell behaviours during beetle embryogenesis correlates with slowing of segmentation. Nature Communications, 6, 6635. doi:10.1038/ncomms7635.

15. Vasiev, B., Balter, A., Chaplain, M., Glazier, J.A., and Weijer, C.J. (2010). Modeling Gastrulation in the Chick Embryo: Formation of the Primitive Streak. PLoS One, 5(5), e10571. doi:10.1371/journal.pone.0010571.

16. Dmitrenok, I., Drobny, V., Johard, L., and Mazzara, M. (2016). Evaluation of spatial trees for simulation of biological tissue. arXiv, 1611.03358.

17. Balzer, M. and Deussen, O. (2005). Voronoi treemaps. IEEE Symposium on Information Visualization, 49–56, Washington, DC.

18. Oroz-Luengo, M.A., Duloquin, L., Castro, C., Savy, T., Faure, E., Lombardo, B., Bourgine, P.., Peyrieras, N., and Santos, A. (2008). Can Voronoi diagram model cell geometries in early sea-urchin embryogenesis? IEEE International Symposium on Biomedical Imaging, Paris, France. doi:10.1109/ISBI.2008.4541043.

19. Horn, M.S., Tobiasz, M., Shen, C. (2009). Visualizing Biodiversity with Voronoi Treemaps. IEEE International Symposium on Visualization and Data, Copenhagen, Denmark. doi:10.1109/ISVD.2009.22.

20. Tian, S., Cui, X., and Gong, Y. (2015). An Approach to Generate Spatial Voronoi Treemaps for Points, Lines, and Polygons. Journal of Electrical and Computer Engineering, 787163, doi:10.1155/2015/787163.

21. Nocaj, A. and Brandes, U. (2012). Computing Voronoi Treemaps: Faster, Simpler, and Resolution-independent. Computer Graphics Forum, 31(3), 855–864 doi:10.1111/j.1467-8659.2012. 03078.x.

22. Bao, Z., Zhao, Z., Boyle, T.J., Murray, J.I., and Waterston, R.H. (2008). Control of Cell Cycle Timing during *C. elegans* Embryogenesis. Developmental Biology, 318(1), 65-72.

23. Shapiro, E., Biezuner, T., and Linnarsson, S. (2013). Single-cell sequencing-based technologies will revolutionize whole-organism science. Nature Reviews Genetics, 14, 618–630.

24. Sammut, M., Cook, S.J., Nguyen, K.C.Q., Felton, T., Hall, D.H., Emmons, S.W., Poole, R.J., and Barrios, A. (2015). Glia-derived neurons are required for sex-specific learning in *C. elegans*. Nature, 526, 385-390.

25. Fay, D.S. (2005). The cell cycle and development: Lessons from *C. elegans*. Seminars in Cell and Developmental Biology, 16, 397–406.

26. Moss, E.G. (2007). Heterochronic Genes and the Nature of Developmental Time. Current Biology, 17(11), R425-R434.

27. Portereiko, M.F. and S.E. Mango (2001). Early Morphogenesis of the *Caenorhabditis elegans* Pharynx. Developmental Biology, 233, 482-494.

28. Ho, V.W.S., Wong, M-K., An, X., Guan, D., Shao, J., Ng, H.C.K., Ren, X., He, K., Liao, J., Ang, Y., Chen, L., Huang, X., Yan, B., Xia, Y., Chan, L.L.H., Chow, K.L., Yan, H., and Zhao, Z. (2015). Systems-level quantification of division timing reveals a common genetic architecture controlling asynchrony and fate asymmetry. Molecular Systems Biology, 11, 814.

29. Schnabel, R., Hutter, H., Moerman, D., and Schnabel, H. (1997). Assessing normal embryogenesis in *Caenorhabditis elegans* using a 4D microscope: variability of development and regional specification. Developmental Biology, 184, 234–265.

30. Duellman, W.E. and Trueb, L. (1994). Biology of Amphibians. Baltimore, Johns Hopkins University Press.

31. Broitman-Maduro, G., Lin, K. T.-H., Hung, W. W. K., & Maduro, M. F. (2006). Specification of the *C. elegans* MS blastomere by the T-box factor TBX-35. Development, 133(16), 3097–3106.

32. Baugh, L.R., Hill, A.A., Slonim, D.K., Brown, E.L., and Hunter, C.P. (2003). Composition and dynamics of the *Caenorhabditis elegans* early embryonic transcriptome. Development, 130(5), 889–900.

33. Tintori, S.C., Osborne Nishimura, E., Golden, P.T., Lieb, J.D., Goldstein, B. (2016). A transcriptional lineage of early *C. elegans* development. Developmental Cell, 38(4), 430-444.

34. Wong, M-K., Guan, D., Ng, K.H.C., Ho, S.V.W. An, X., Li, R., Ren, X., and Zhao, X.Z. (2016). Timing of Tissue-specific Cell Division Requires a Differential Onset of Zygotic Transcription during Metazoan Embryogenesis. Journal of Biological Chemistry, 291(24), 12501–12513.

35. Stout, R.F., Verkhratsky, A., and Parpura, V. (2014). *Caenorhabditis elegans* glia modulate neuronal activity and behavior. Frontiers in Cellular Neuroscience, 8, 67.

36. Velarde, N., Gunsalus, K.C., and Piano, F. (2007). Diverse roles of actin in *C. elegans* early embryogenesis. BMC Developmental Biology, 7, 142.

37. Chisholm, A.D. and Hardin, J. Epidermal Morphogenesis (2005), WormBook: the online review of *C. elegans* biology. Accessed on March 11, 2018, http://wormbook.org/chapters/www_epidermalmorphogenesis/epidermalmorphogenesis.pdf.

38. Luo, L., Wen, Q., Ren, J., Hendricks, M., Gershow, M., Qin, Y., Greenwood, J., Soucy, E.R., Klein, M., Smith-Parker, H.K., Calvo, A.C., Colón-Ramos, D.A., Samuel, A.D., and Zhang, Y. (2014). Dynamic encoding of perception, memory, and movement in a *C. elegans* chemotaxis circuit. Neuron. 82(5), 1115-1128.